AIAA JOURNAL
Vol. 46, No. 12, December 2008

Analysis of Constrained Damping Layers, Including Normal-Strain Effects

Shing-Jia Tang*
University of Tennessee, Knoxville, Tennessee 37996
and
Arnold Lumsdaine†
Agilent Technologies, Oak Ridge, Tennessee 37830

DOI: 10.2514/1.33068

A beam partially covered with a constrained damping layer is analyzed. The longitudinal normal strain and shear strain in the viscoelastic layer are considered. Hamilton's principle is used to derive equations of motion and boundary conditions. A sixth-order equation is used to describe the portion of the beam covered with a constrained damping layer. The characteristic equations are solved numerically to determine normalized natural frequency and loss factor values. The loss parameter (normalized loss factor) is shown to be a function of the shear parameter g_T; the geometric parameter Y_T; the normalized coverage length L_C/L; dimensionless coefficients B_1, B_2, and B_3; and the core loss factor η_2. It is shown that traditional constrained-layer damping theory that includes only shearing in the damping layer is inadequate for very small or very large values of the shear parameter. Optimal shear-parameter and coverage-length values are determined for a variety of boundary conditions. Results demonstrate the optimal values for the shear parameter and coverage length to obtain maximum damping levels. Plots are derived to determine the optimal coverage length for any shear-parameter value for maximum loss factor.

Nomenclature

A_i = area of cross section of the constrained and base layers
c = distance between face layers, $h_1 + 2h_2 + h_3$
D = combined flexural rigidity
D^* = combined flexural rigidity
E_i = Young's modulus of the constrained and base layers
E_2^* = Young's modulus of the viscoelastic layer
G_2 = real part of the core complex shear modulus, $G_2^* = G_2(1 + j\eta_2)$
g = shear parameter
h_i = half-thickness of the constrained and damping layers
I_i = area moment of inertia of the constrained, damping, and base layers about its own midline
i = index
j = $(-1)^{1/2}$
k^* = complex characteristic value
L = length of base layer
m = mass per unit length of beam
T = kinetic energy
t = time
u = shear-strain measure
u_i = axial displacement of the central line of the constrained, damping, and base layers
V = potential energy
w = vertical deflection
Y^* = geometric parameter
γ_2 = shear strain in the core
η = system loss factor
$\bar{\eta}$ = loss parameter
η_2 = core loss factor
Ω = resonant frequency
$\bar{\Omega}$ = frequency parameter
Ω^* = complex natural frequency

Received 25 June 2007; revision received 15 May 2008; accepted for publication 15 May 2008.

*Graduate Research Assistant, Department of Mechanical, Aerospace, and Biomedical Engineering; shingjia@hotmail.com.
†Research and Development Manager, 701 Scarboro Road, Suite 100; alumsdaine@gmail.com.

I. Introduction

CONSTRAINED damping layers are commonly used as a means for vibration and noise control. It is usually assumed that energy is dissipated exclusively through shear deformation in the viscoelastic material. The assumption is valid when the viscoelastic layer is of moderate stiffness. However, when the viscoelastic material is stiffer, the longitudinal stress also must be considered.

Kerwin [1] first discussed a three-layer beam with a damping layer sandwiched between two elastic layers. DiTaranto [2] derived a sixth-order differential equation to describe the transverse motion of a constrained laminated beam. Mead and Markus [3] developed a sixth-order differential equation of motion in terms of transverse displacement for arbitrary boundary conditions and developed boundary conditions beyond those described by DiTaranto [2]. Mead and Markus [4] also solved these equations for fixed–fixed, free–free, and simply supported beams. Yan and Dowell [5] performed an analysis including longitudinal and rotary inertia in all layers and shear strain in the outer layers. Fasana and Marchesiello [6] predicted loss factors by means of the Rayleigh–Ritz method. All of these analytical models only include the shear deformation of the viscoelastic damping layer. Lee and Kim [7,8] analyzed sandwich plates that include shear strain and transverse normal strain in the viscoelastic layer. Miles and Reinhall [9] analyzed sandwich beams that include shear and thickness deformation in the viscoelastic layer. Some results obtained using finite element analysis include normal strains in the viscoelastic layer (both lateral and longitudinal). Soni and Bogner [10] used a commercial finite element code to determine the damping properties of a constrained-layer structure, modeling the damping layers with solid elements and the elastic layers with shell elements. Wang and Wereley [11] used spectral finite elements to analyze passive constrained-layer damping structures in which the longitudinal inertia of the base beam and constraining layer was included.

The desire to maximize the damping properties of constrained-layer structures has led to studies in optimization. Lall et al. [12] performed optimum design for simply supported sandwich panels, maximizing the loss factor with the layer densities, thicknesses, and temperature being among the design variables. An advantage of examining the simply supported case is the availability of a

closed-form solution. Lifshitz and Leibowitz [13] performed optimal design for maximum viscoelastic damping. Lumsdaine and Scott [14] minimized the peak displacement in beams and plates by optimizing the heights of the constrained damping layers. The finite element model used solid elements for all layers.

The preceding optimization studies assumed a fully covered sandwich structure. To minimize mass and achieve a better damping effect, a partially covered sandwich beam has also been studied by many investigators. Markus [15] derived an expression for the loss factor of beams with partial coverage. He examined only simply supported beams partially covered in the central portion. Nokes and Nelson [16] performed a theoretical and experimental study for a symmetrically placed constrained patch for symmetric boundary conditions. Plunkett and Lee [17] considered the same problem to optimize the length of the damping layer. Lall et al. [18] studied partially covered sandwich beams using three methods: two numerical methods (one developed by Markus [15] and the other using a Rayleigh–Ritz formulation) and one exact method [4]. This analysis was also performed for a simply supported beam. Mantena et al. [19] determined the loss factor of cantilever beams partially covered using finite element modeling, calculating the loss factor with the modal-strain-energy method. These results were confirmed experimentally. They showed that a partially covered beam could have a higher loss factor than a fully covered beam. Chen and Levy [20,21] analyzed a partially covered double-sandwich cantilever beam (with constrained damping layers on both sides of the beam). Kung and Singh [22] performed an analysis using the energy method for the harmonic vibration response of a beam with multiple passive constrained-layer damping (PCLD) patches. Austin and Inman [23] showed that the use of the Mead–Markus model had some limitations. They showed that the beam should be thin and the length of the constraining layer cannot be too short. Ro and Baz [24] optimized the placement of an active constrained damping patch (with a piezoelectric actuator as the constraining layer) for minimum weight, modeling the structure with finite elements and using the modal-strain-energy method to compute the loss factor. Tang and Lumsdaine [25] performed an optimization analysis for fixed–fixed and fixed–pinned beams.

To the authors' knowledge, no previous work has developed and solved analytic equations of motion for a partially covered beam with a variety of boundary conditions for which normal strain in the length direction in the viscoelastic layer is considered. In this work, these equations of motion are developed and solved numerically. The resulting loss parameter (normalized loss factor) is found to be a function of seven nondimensional parameters: the shear parameter g_N; the geometric parameter Y_N; the normalized coverage length L_C/L; coefficients B_1, B_2, and B_3; and the core loss factor η_2. Results show that for most beams, the highest level of damping is achieved with less than full coverage of the constraining layer ($L_C/L < 1$). The optimal length of the constraining layer is determined for different values of the shear parameter, the loss parameter, and the core loss factor. These results are graphed for easy use in designing a layer with optimal damping. Crassidis et al. [26] analyzed hybrid treatments which combined active constrained-layer damping and PCLD. The results presented in this work could be used to optimize the PCLD portion from their work. The normal strain in the damping layer is important to include in cases in which the shear modulus in the layer is large.

II. Analytical Formulation

A laminated cantilever beam consists of a constraining layer, damping layer, and base layer, as shown in Fig. 1. This has been shown to produce higher damping levels than when the constraining layer is left free [19]. The constraining layer and base layer are assumed to be purely elastic, with Young's moduli of E_1 and E_3, respectively. The damping layer is viscoelastic with a complex dynamic modulus $E_2^* = E_2(1 + j\eta_2)$ and shear modulus $G_2^* = (1 + j\eta_2)$. The core loss factor is assumed to be the same for both the elastic and shear moduli (i.e., Poisson's ratio is assumed to be frequency-invariant).

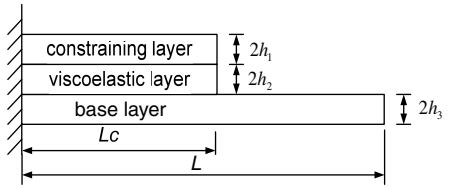

Fig. 1 Partially covered laminated beam.

The following assumptions are made in the analysis:

1) The beam deflection is small and uniform across any section.

2) There is no slipping between the elastic and viscoelastic layers at their interfaces.

3) The elastic layers displace laterally the same amount.

4) The longitudinal and rotary inertial effects of the beam are negligible.

5) Shear strains in the elastic layers are negligible.

Hamilton's principle is used to derive the equations of motion and boundary conditions. The beam is separated into two regions, as shown in Fig. 2.

The external work, kinetic energy, and potential energy for the covered region can be expressed as follows:

$$W = M\frac{\partial w}{\partial x} - Sw \tag{1}$$

$$T = \frac{1}{2}\int m\left(\frac{\partial w}{\partial t}\right)^2 \mathrm{d}x \tag{2}$$

$$(V_1 + V_2 + V_3)_{\text{bending}} = \frac{1}{2}\int\left[E_1 I_1\left(\frac{\partial^2 w}{\partial x^2}\right)^2 + \frac{E_2^* I_2}{(1-\nu^2)}\left(\frac{\partial^2 w}{\partial x^2} - \frac{\partial \gamma_2}{\partial x}\right)^2 + E_3 I_3\left(\frac{\partial^2 w}{\partial x^2}\right)^2\right]\mathrm{d}x \tag{3}$$

$$(V_1 + V_2 + V_3)_{\text{extension}} = \frac{1}{2}\int\left[E_1 A_1\left(\frac{\partial u_1}{\partial x}\right)^2 + \frac{E_2^* A_2}{(1-\nu^2)}\left(\frac{\partial u_2}{\partial x}\right)^2 + E_3 A_3\left(\frac{\partial u_3}{\partial x}\right)^2\right]\mathrm{d}x \tag{4}$$

$$(V_2)_{\text{shearing}} = \frac{1}{2}\int G_2^* A_2 \gamma_2^2 \mathrm{d}x \tag{5}$$

Because of the assumption that the elastic layers have the same lateral deformation, the transverse normal strain in the viscoelastic layer is zero. The plane stress constitutive relationship produces the $1 - \nu^2$ term in the denominator of Eqs. (3) and (4). The external work, kinetic energy, and potential energy for the uncovered region can be expressed as follows:

$$\begin{aligned} W &= -M\frac{\partial w_u}{\partial x} + Sw_u \\ T &= \frac{1}{2}\int m_3\left(\frac{\partial w_u}{\partial t}\right)^2 \mathrm{d}x \\ V &= \frac{1}{2}\int E_3 I_3\left(\frac{\partial^2 w_u}{\partial x^2}\right)^2 \mathrm{d}x \end{aligned} \tag{6}$$

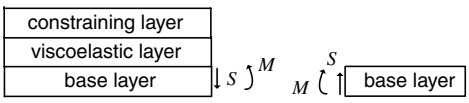

Fig. 2 Internal loading of each part of beam.

where w and w_u are the vertical deflections of the beam for the covered region and uncovered region, respectively; u_1 and u_3 are the axial displacements of the midplane of the elastic layers; u_2 is the axial displacement of the midplane of the damping layer; and γ_2 is the shear strain in the damping layer. Looking at Fig. 3, it can be shown that u_1, u_2, u_3, and $\partial w/\partial x$ are related through

$$u_1 - u_2 = (h_1 + h_2)\frac{\partial w}{\partial x} - h_2\gamma_2 \tag{7}$$

$$u_1 - u_3 = c\frac{\partial w}{\partial x} - 2h_2\gamma_2 \tag{8}$$

From the force equilibrium, we can obtain

$$E_1A_1\frac{\partial u_1}{\partial x} + \frac{E_2^*A_2}{(1-\nu^2)}\frac{\partial u_2}{\partial x} + E_3A_3\frac{\partial u_3}{\partial x} = 0 \tag{9}$$

The terms $\partial u_1/\partial x$, $\partial u_2/\partial x$, and $\partial u_3/\partial x$ can be solved from Eqs. (7–9) and substituted into Eq. (4). A variable $u = 2h_2L\gamma_2/c$ may then be defined. The energy terms for the covered region can be expressed as

$$T = \frac{1}{2}\frac{D^*}{L^3}\int\frac{mL^4}{D^*}\left(\frac{\partial w}{\partial t}\right)^2 \mathrm{d}\bar{x} \tag{10}$$

$$\begin{aligned} V = {} & \frac{1}{2}\frac{D^*}{L^3}\int\left[\left(\frac{\partial^2 w}{\partial \bar{x}^2}\right)^2 - 2\frac{E_2^*I_2c}{2h_2D^*(1-\nu^2)}\frac{\partial^2 w}{\partial \bar{x}^2}\frac{\partial u}{\partial \bar{x}}\right. \\ & \left. + \frac{E_2^*I_2c^2}{4h_2^2D^*(1-\nu^2)}\left(\frac{\partial u}{\partial \bar{x}}\right)^2\right]\mathrm{d}\bar{x} + \frac{1}{2}\frac{D^*}{L^3}\int\left\{Y_T^*\left(\frac{\partial^2 w}{\partial \bar{x}^2} - \frac{\partial u}{\partial \bar{x}}\right)^2\right. \\ & + \frac{E_2^*A_2}{E_1A_1(1-\nu^2)}\left(\frac{h_2+h_3}{c}\right)^2 Y_T^*\left[\frac{\partial^2 w}{\partial \bar{x}^2} - \frac{c}{2(h_2+h_3)}\frac{\partial u}{\partial \bar{x}}\right]\Bigg\}\mathrm{d}\bar{x} \\ & + \frac{1}{2}\frac{D^*}{L^3}\int\left\{\frac{E_2^*A_2}{E_3A_3(1-\nu^2)}\left(\frac{h_1+h_2}{c}\right)^2 Y_T^*\left[\frac{\partial^2 w}{\partial \bar{x}^2} - \frac{c}{2(h_1+h_2)}\frac{\partial u}{\partial \bar{x}}\right]\right. \\ & \left. + g_T^*Y_T^*u^2\right\}\mathrm{d}\bar{x} \end{aligned} \tag{11}$$

The energy terms for the uncovered region can be expressed as

$$T = \frac{1}{2}\frac{D^*}{L^3}\int\frac{m_3L^4}{D^*}\left(\frac{\partial w_u}{\partial t}\right)^2\mathrm{d}\bar{x} \qquad V = \frac{1}{2}\frac{D^*}{L^3}\int\frac{E_3I_3}{D^*}\left(\frac{\partial^2 w_u}{\partial \bar{x}^2}\right)^2\mathrm{d}\bar{x} \tag{12}$$

where g_T^* and Y^* are defined as

$$g_T^* = \frac{G_2^*A_2L^2(E_1A_1 + E_2^*A_2/(1-\nu^2) + E_3A_3)}{4h_2^2E_1A_1E_3A_3} \tag{13}$$

$$Y_T^* = \frac{c^2E_1A_1E_3A_3}{D^*(E_1A_1 + E_2^*A_2/(1-\nu^2) + E_3A_3)} \tag{14}$$

$D^* = E_1I_1 + E_2^*I_2/(1-\nu^2) + E_3I_3$ is the combined flexural rigidity, and $\bar{x} = x/L$ is the normalized length.

Applying Hamilton's principle, equations of motion may be obtained:

$$\frac{mL^4}{D^*}\frac{\partial^2 w}{\partial t^2} + B_1\frac{\partial^4 w}{\partial \bar{x}^4} - B_2\frac{\partial^3 u}{\partial \bar{x}^3} = 0 \tag{15}$$

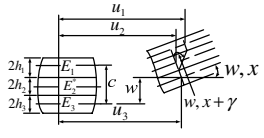

Fig. 3 Deformed shape of beam to establish relationship between u_1, u_3 and $\partial w_1/\partial x$.

$$B_2\frac{\partial^3 w}{\partial \bar{x}^3} - B_3\frac{\partial^2 u}{\partial \bar{x}^2} + Y_T^*g_T^*u = 0 \tag{16}$$

$$m_3L^4\frac{\partial^2 w_u}{\partial t^2} + E_3I_3\frac{\partial^4 w_u}{\partial \bar{x}^4} = 0 \tag{17}$$

where nondimensional parameters B_1, B_2, and B_3 are defined as

$$\begin{aligned} B_1 = {} & 1 + \left[1 + \frac{E_2^*A_2}{E_1A_1(1-\nu^2)}\left(\frac{h_2+h_3}{c}\right)^2\right. \\ & \left. + \frac{E_2^*A_2}{E_3A_3(1-\nu^2)}\left(\frac{h_1+h_2}{c}\right)^2\right]Y_T^* \\ B_2 = {} & \frac{E_2^*I_2c}{2h_2D^*(1-\nu^2)} + \left[1 + \frac{E_2^*A_2}{2E_1A_1(1-\nu^2)}\left(\frac{h_2+h_3}{c}\right)\right. \\ & \left. + \frac{E_2^*A_2}{2E_3A_3(1-\nu^2)}\left(\frac{h_1+h_2}{c}\right)\right]Y_T^* \\ B_3 = {} & \frac{E_2^*I_2c^2}{4h_2^2D^*(1-\nu^2)} + \left(1 + \frac{E_2^*A_2}{4E_1A_1(1-\nu^2)}\right. \\ & \left. + \frac{E_2^*A_2}{4E_3A_3(1-\nu^2)}\right)Y_T^* \end{aligned}$$

Equations (15) and (16) may be combined into one equation in terms of w only.

$$\begin{aligned} & (B_1B_3 - B_2^2)\frac{\partial^6 w}{\partial \bar{x}^6} - B_1Y_T^*g_T^*\frac{\partial^4 w}{\partial \bar{x}^4} \\ & + \frac{mL^4}{D^*}\frac{\partial^2}{\partial t^2}\left(B_3\frac{\partial^2}{\partial \bar{x}^2} - Y_T^*g_T^*\right)w = 0 \end{aligned} \tag{18}$$

The boundary conditions for the covered region are as follows:

$$-\left(B_1\frac{\partial^2 w}{\partial \bar{x}^2} - B_2\frac{\partial u}{\partial \bar{x}}\right) + \frac{ML^2}{D^*} = 0 \quad \text{or} \quad \frac{\partial w}{\partial \bar{x}} = 0 \tag{19}$$

$$\left(B_1\frac{\partial^3 w}{\partial \bar{x}^3} - B_2\frac{\partial^2 u}{\partial \bar{x}^2}\right) - \frac{SL^3}{D^*} = 0 \quad \text{or} \quad w = 0 \tag{20}$$

$$N = B_2\frac{\partial^2 w}{\partial \bar{x}^2} - B_3\frac{\partial u}{\partial \bar{x}} = 0 \quad \text{or} \quad u = 0 \tag{21}$$

The boundary conditions for the uncovered region are as follows:

$$-\frac{E_3I_3}{D^*}\frac{\partial^2 w_u}{\partial \bar{x}^2} - \frac{ML^2}{D^*} = 0 \quad \text{or} \quad \frac{\partial w_u}{\partial \bar{x}} = 0 \tag{22}$$

$$\frac{E_3I_3}{D^*}\frac{\partial^3 w_u}{\partial \bar{x}^3} + \frac{SL^3}{D^*} = 0 \quad \text{or} \quad w_u = 0 \tag{23}$$

Equations (19–21) may be expressed in terms of w only:

$$\begin{aligned} & \left[-(B_1B_3 - B_2^2)\frac{\partial^4 w}{\partial \bar{x}^4} + B_1Y_T^*g_T^*\frac{\partial^2 w}{\partial \bar{x}^2} - \frac{mL^4}{D}B_2\frac{\partial^2 w}{\partial t^2}\right] \\ & - \frac{MY_T^*g_T^*L^2}{D^*} = 0 \end{aligned} \tag{24}$$

$$\left[-(B_1B_3-B_2^2)\frac{\partial^5 w}{\partial \bar{x}^5}+B_1Y_T^*g_T^*\frac{\partial^3 w}{\partial \bar{x}^3}-\frac{mL^4}{D}B_2\frac{\partial^3 w}{\partial t^2\partial \bar{x}}\right] - \frac{SY_T^*g_T^*L^3}{D^*}=0 \tag{25}$$

$$N=(B_1B_3-B_2^2)\frac{\partial^4 w}{\partial \bar{x}^4}-B_2Y_T^*g_T^*\frac{\partial^2 w}{\partial \bar{x}^2}+\frac{mL^4}{D}B_3\frac{\partial^2 w}{\partial t^2}=0 \tag{26}$$

Equations (22) and (24) may be reduced to one equation:

$$\frac{D^*}{Y_T^*g_T^*L^2}\left[-(B_1B_3-B_2^2)\frac{\partial^4 w}{\partial \bar{x}^4}+B_1Y_T^*g_T^*\frac{\partial^2 w}{\partial \bar{x}^2}-\frac{mL^4}{D}B_2\frac{\partial^2 w}{\partial t^2}\right] - \frac{E_3I_3}{L^2}\frac{\partial^2 w_u}{\partial \bar{x}^2}=0 \tag{27}$$

And Eqs. (23) and (25) may be reduced to one equation:

$$\frac{D^*}{Y_T^*g_T^*L^3}\left[-(B_1B_3-B_2^2)\frac{\partial^5 w}{\partial \bar{x}^5}+B_1Y_T^*g_T^*\frac{\partial^3 w}{\partial \bar{x}^3}-\frac{mL^4}{D}B_2\frac{\partial^3 w}{\partial t^2\partial \bar{x}}\right] - \frac{E_3I_3}{L^3}\frac{\partial^3 w_u}{\partial \bar{x}^3}=0 \tag{28}$$

Two more boundary equations are necessary. At the conjunction, geometry continuity should be met. The displacement and slope should be the same at the interface. Thus, the two additional boundary equations may be written as

$$w|_{\bar{x}=\frac{L_C}{L}}=w_u|_{\bar{x}=\frac{L_C}{L}} \qquad \left.\frac{\partial w}{\partial \bar{x}}\right|_{\bar{x}=\frac{L_C}{L}}=\left.\frac{\partial w_u}{\partial \bar{x}}\right|_{\bar{x}=\frac{L_C}{L}} \tag{29}$$

There are many possible boundary conditions for a laminated beam. They are given in Table 1.

If E_2^* is set to zero, the preceding equations of motion and boundary conditions for the covered region can be reduced to the following:

$$\frac{mL^4}{D}\frac{\partial^2 w}{\partial t^2}+(1+Y)\frac{\partial^4 w}{\partial \bar{x}^4}-Y\frac{\partial^3 u}{\partial \bar{x}^3}=0 \tag{30}$$

$$Y\frac{\partial^3 w}{\partial \bar{x}^3}-Y\frac{\partial^2 u}{\partial \bar{x}^2}+Yg^*u=0 \tag{31}$$

$$\frac{\partial^6 w}{\partial \bar{x}^6}-(1+Y)g^*\frac{\partial^4 w}{\partial \bar{x}^4}+\frac{mL^4}{D}\frac{\partial^2}{\partial t^2}\left(\frac{\partial^2}{\partial \bar{x}^2}-g^*\right)w=0 \tag{32}$$

$$M=\frac{D}{L^2g^*}\left[-\frac{\partial^4 w}{\partial \bar{x}^4}+(1+Y)g^*\frac{\partial^2 w}{\partial \bar{x}^2}-\frac{mL^4}{D}\frac{\partial^2 w}{\partial t^2}\right]=0 \tag{33}$$

$$S=\frac{D}{L^3g^*}\left[-\frac{\partial^5 w}{\partial \bar{x}^5}+(1+Y)g^*\frac{\partial^3 w}{\partial \bar{x}^3}-\frac{mL^4}{D}\frac{\partial^3 w}{\partial t^2\partial \bar{x}}\right]=0 \tag{34}$$

Table 1 Possible boundary conditions

End arrangements	Boundary conditions
Free-unrestrained	$(B_1B_3-B_2^2)w^{\mathrm{IV}}-B_2Y^*g^*w^{\mathrm{II}}-mL^4B_3\Omega^{*2}w/D^*=0$
	$(B_1B_3-B_2^2)w^{\mathrm{IV}}-B_1Y^*g^*w^{\mathrm{II}}-(mL^4/D^*)B_2\Omega^{*2}w=0$
	$(B_1B_3-B_2^2)w^{\mathrm{V}}-B_1Y^*g^*w^{\mathrm{III}}-(mL^4/D^*)B_2\Omega^{*2}w^{\mathrm{I}}=0$
Free-riveted	$(B_1B_3-B_2^2)w^{\mathrm{IV}}-B_1Y^*g^*w^{\mathrm{II}}-(mL^4/D^*)B_2\Omega^{*2}w=0$
	$(B_1B_3-B_2^2)w^{\mathrm{V}}-B_1Y^*g^*w^{\mathrm{III}}-\frac{mL^4}{D^*}B_2\Omega^{*2}w^{\mathrm{I}}=0$
	$(B_1B_3-B_2^2)w^{\mathrm{V}}-B_2Y^*g^*w^{\mathrm{III}}-(mL^4/D^*)B_3\Omega^{*2}w^{\mathrm{I}}=0$
Pinned-unrestrained	$w=0$
	$w^{\mathrm{II}}=0$
	$w^{\mathrm{IV}}=0$
Pinned-riveted	$w=0$
	$(B_1B_3-B_2^2)w^{\mathrm{IV}}-B_1Y^*g^*w^{\mathrm{II}}=0$
	$(B_1B_3-B_2^2)w^{\mathrm{V}}-B_2Y^*g^*w^{\mathrm{III}}-(mL^4/D^*)B_3\Omega^{*2}w^{\mathrm{I}}=0$
Clamped-unrestrained	$w=0$
	$w^{\mathrm{I}}=0$
	$(B_1B_3-B_2^2)w^{\mathrm{IV}}-B_2Y^*g^*w^{\mathrm{II}}=0$
Sliding-unrestrained	$w^{\mathrm{I}}=0$
	$(B_1B_3-B_2^2)w^{\mathrm{IV}}-B_2Y^*g^*w^{\mathrm{II}}-(mL^4/D^*)B_3\Omega^{*2}w=0$
	$(B_1B_3-B_2^2)w^{\mathrm{V}}-B_1Y^*g^*w^{\mathrm{III}}=0$

Table 2 Dimensions and material properties for validation study

	Elastic layers	
Young's modulus	$E_1=E_3=6.9\times10^{10}$ N/m^2	
Density	$\rho_1=\rho_3=2800$ kg/m^3	[a]$\rho_1=\rho_3=2766$ kg/m^3
Thickness	$h_1=h_3=0.76$ mm	[a]$h_1=h_3=0.762$ mm
	Viscoelastic layer	
Young's modulus	$E_2=1.794\times10^6$ N/m^2	$E_2=1.794\times10^6$ N/m^2
Poisson's ratio	$\upsilon=0.3$	
Density	$\rho_2=968.3$ kg/m^3	[a]$\rho_2=968.1$ kg/m^3
Thickness	$h_2=0.0635$ mm	
Core loss factor	$\eta_2=0.1, 0.2, 0.3, 0.6, 1.0, 1.5$	
	Whole beam	
Length	$L=177.8$ mm	
Width	$w=12.7$ mm	

[a]Used by [25,27].

$$N = \frac{\partial^4 w}{\partial \bar{x}^4} - Y g^* \frac{\partial^2 w}{\partial \bar{x}^2} + \frac{\partial^2 w}{\partial t^2} = 0 \tag{35}$$

where g^*, Y, and D are defined as [4]

$$g^* = \frac{G_2^* A_2 L^2 (E_1 A_1 + E_3 A_3)}{4 h_2^2 E_1 A_1 E_3 A_3} = g(1 + j\eta_2)$$

where g is the shear parameter,

$$Y = \frac{c^2 E_1 A_1 E_3 A_3}{D(E_1 A_1 + E_3 A_3)} \qquad D = E_1 I_1 + E_3 I_3 \tag{36}$$

where Y is the geometric parameter.

So if the longitudinal normal strain is ignored, the equations reduce the traditional forms of the equations given by Mead and Markus [3].

Table 3 Natural frequency values

η_2	Analysis	Mode 1	Mode 2	Mode 3	Mode 4	Mode 5	Mode 6
0.1	[a]	64.075	296.41	743.7	1393.9	2261.09	——
	[b]	64.2	297.0	747.2	1408.3	2304.0	——
	[c]	60.9	288.8	732.9	1381.4	2246.6	——
	[d]	63.35	292.1	732.8	1373	——	——
	[e]	63.61	294.20	738.02	1383.06	2243.21	——
	[f]	63.607	294.22	738.08	1383.27	2243.68	3317.77
	[g]	63.607	294.22	738.08	1383.27	2243.68	3317.77
	[h]	64.1	296.4	743.7	1393.9	2261.1	3343.6
	[i]	64.1	296.8	745.8	——	——	——
	[j]	64.129	296.67	744.33	1395.13	2263.02	3346.46
	[k]	64.129	296.67	744.33	1395.13	2263.02	3346.46
0.2	[a]	64.21	296.64	743.85	1394.0	2261.15	——
	[b]	64.4	297.6	748.0	1409.0	2304.0	——
	[c]	61.2	289.0	733.4	1381.7	2246.9	——
	[d]	——	——	——	——	——	——
	[e]	63.74	294.43	738.18	1383.14	2243.27	——
	[j]	63.740	294.447	738.236	1383.36	2243.74	3317.81
	[k]	63.740	294.447	738.236	1383.36	2243.74	3317.81
0.3	[a]	64.43	297.01	744.1	1394.0	2261.24	——
	[b]	64.7	298.0	748.2	1409.5	2305.0	——
	[c]	61.5	289.8	734.0	1382.3	2247.2	——
	[d]	——	——	——	——	——	——
	[e]	63.957	294.796	738.432	1383.283	2243.357	——
	[f]	63.957	294.816	738.492	1383.496	2243.832	3317.87
	[g]	63.957	294.816	738.492	1383.496	2243.832	3317.87
	[h]	64.4	297	744.1	1394	2261.2	3343.7
	[j]	64.482	297.267	744.743	1395.351	2263.171	3346.56
	[k]	64.482	297.267	744.743	1395.351	2263.171	3346.56
0.6	[a]	65.48	298.9	758.48	1394.9	2261.7	——
	[b]	65.5	301.0	753.0	1414.0	2310.0	——
	[c]	62.7	292.4	737.4	1385.2	2249.7	——
	[d]	——	——	——	——	——	——
	[e]	65.005	296.675	739.793	1384.016	2243.847	——
	[f]	65.005	296.696	739.854	1384.234	2244.326	3318.19
	[g]	65.005	296.696	739.854	1384.234	2244.326	3318.19
	[h]	65.5	298.9	745.5	1394.9	2261.7	3344
	[j]	65.538	299.159	746.112	1396.092	2263.667	3346.89
	[k]	65.538	299.159	746.112	1396.092	2263.667	3346.89
1.0	[a]	67.41	302.8	748.6	1396.6	2262.88	——
	[b]	67.4	307.0	762.0	1422.0	2316.0	——
	[c]	64.3	296.7	744.3	1391.0	2254.8	——
	[d]	——	——	——	——	——	——
	[e]	66.913	300.533	742.92	1385.684	2244.98	——
	[f]	66.913	300.556	742.983	1385.912	2245.468	3318.93
	[g]	66.913	300.556	742.983	1385.912	2245.468	3318.94
	[h]	67.4	302.8	748.6	1396.6	2262.9	3345
	[j]	67.463	303.045	749.255	1397.778	2264.813	3347.63
	[k]	67.463	303.045	749.255	1397.778	2264.813	3347.63
1.5	[a]	69.88	308.85	754.0	1399.7	2265.0	——
	[b]	70.0	315.0	774.0	1433.0	2328.0	——
	[c]	64.4	303.5	755.3	1400.6	2263.8	——
	[d]	69.13	304.3	743.4	1378	——	——
	[e]	69.366	306.555	748.725	1388.773	2247.120	——
	[f]	69.366	306.582	748.792	1389.017	2247.623	3320.32
	[g]	69.366	306.582	748.792	1389.017	2247.623	3320.32
	[h]	69.9	308.9	754	1399.7	2265	3346
	[j]	69.937	309.111	755.090	1400.895	2266.98	3349.02
	[k]	69.937	309.111	755.090	1400.895	2266.98	3349.02

[a]Calculated from [27]. [b]Result from [24]. [c]Result from [25]. [d]Result from [7]. [e]Result from [27]. [f]E^* is set to zero. [g]Present theory.
[h]Result from [23]. [i]Result from [28]. [j]E^* is set to zero. [k]Present theory.

If shear strain in the viscoelastic layer is neglected, the equation of motion is as follows:

$$\frac{mL^4}{D^*}\frac{\partial^2 w}{\partial t^2} + (EI)_N \frac{\partial^4 w}{\partial \bar{x}^4} = 0$$
$$(EI)_N = 1 + \left[1 + \frac{E_2^* A_2}{E_1 A_1 (1-\nu^2)}\left(\frac{h_2 + h_3}{c}\right) + \frac{E_2^* A_2}{E_3 A_3 (1-\nu^2)}\left(\frac{h_1 + h_2}{c}\right)\right] Y_T^* \tag{37}$$

III. Solution

Displacements w and w_u may be expressed as

$$w = Ae^{k^*\bar{x}}e^{j\Omega^* t} \qquad w_u = Be^{k^*\bar{x}}e^{j\Omega^* t} \tag{38}$$

where Ω^* and k^* are complex natural frequency and characteristic values to be determined. Substituting Eq. (38) into Eqs. (17) and (18) yields:

Table 4 Loss-parameter values

η_2	Analysis	Mode 1	Mode 2	Mode 3	Mode 4	Mode 5	Mode 6
0.1	[a]	2.815	2.424	1.54	0.889	0.573	——
	[b]	2.817	2.425	1.534	0.878	0.559	——
	[c]	2.646	2.173	1.328	0.742	0.463	——
	[d]	2.86	2.43	1.54	0.89	——	——
	[e]	2.81	2.43	1.54	0.89	0.574	——
	[f]	2.8132	2.427	1.544	0.891	0.574	0.391
	[g]	2.8132	2.427	1.544	0.891	0.574	0.391
	[h]	2.82	2.42	1.54	0.89	0.57	0.39
	[i]	2.81	2.42	1.53	——	——	——
	[j]	2.815	2.424	1.541	0.889	0.573	0.390
	[k]	2.815	2.424	1.541	0.889	0.573	0.390
0.2	[a]	5.56	4.83	3.08	1.776	1.144	——
	[b]	5.564	4.832	3.066	1.756	1.118	——
	[c]	5.292	4.346	2.656	1.484	0.926	——
	[d]	——	——	——	——	——	——
	[e]	5.56	4.83	3.09	1.78	1.14	——
	[j]	5.556	4.834	3.086	1.782	1.148	0.783
	[k]	5.556	4.834	3.086	1.782	1.148	0.783
0.3	[a]	8.169	7.197	4.614	2.664	1.716	——
	[b]	8.175	7.203	4.593	2.634	1.68	——
	[c]	7.938	6.519	3.984	2.226	1.389	——
	[d]	——	——	——	——	——	——
	[e]	8.165	7.204	4.622	2.670	1.720	——
	[f]	8.165	7.205	4.6228	2.672	1.722	1.174
	[g]	8.165	7.205	4.6228	2.672	1.722	1.174
	[h]	8.25	7.14	4.62	2.67	1.71	1.171
	[j]	8.170	7.197	4.613	2.665	1.717	1.171
	[k]	8.170	7.197	4.613	2.665	1.717	1.171
0.4	[a]	14.76	13.938	9.168	5.316	3.432	——
	[b]	14.772	13.956	9.126	5.256	3.36	——
	[c]	15.876	13.038	7.968	4.452	2.778	——
	[d]	——	——	——	——	——	——
	[e]	14.750	13.949	9.178	5.326	3.437	
	[f]	14.750	13.952	9.180	5.329	3.439	2.346
	[g]	14.750	13.952	9.180	5.329	3.439	2.346
	[h]	14.76	13.92	9.18	5.34	3.42	2.34
	[j]	14.761	13.938	9.161	5.316	3.430	2.340
	[k]	14.761	13.938	9.161	5.316	3.430	2.340
1.0	[a]	20.22	21.77	15.02	8.81	5.7	——
	[b]	20.19	21.8	15	8.73	5.6	——
	[c]	26.46	21.72	13.28	7.42	4.63	——
	[d]	——	——	——	——	——	——
	[e]	20.202	21.72	15.023	8.828	5.714	——
	[f]	20.202	21.790	15.055	8.833	5.717	3.905
	[g]	20.202	21.790	15.055	8.833	5.717	3.905
	[h]	20.2	21.8	15	8.8	5.7	3.9
	[j]	20.220	21.768	15.025	8.811	5.702	3.894
	[k]	20.220	21.768	15.025	8.811	5.702	3.894
1.5	[a]	22.956	29.625	21.9	13.095	8.52	——
	[b]	22.83	29.28	21.855	13.02	8.385	——
	[c]	26.46	32.58	19.92	10.86	6.945	——
	[d]	23.4	29.6	21.9	13.1	——	——
	[e]	22.938	29.651	21.931	13.122	8.534	——
	[f]	22.938	29.655	21.934	13.128	8.538	5.843
	[g]	22.938	29.655	21.934	13.128	8.538	5.844
	[h]	22.95	29.55	21.9	13.05	8.55	5.85
	[j]	22.964	29.629	21.893	13.095	8.516	5.827
	[k]	22.964	29.629	21.893	13.095	8.516	5.827

[a]Calculated from [27]. [b]Result from [24]. [c]Result from [25]. [d]Result from [7]. [e]Result from [27]. [f]E^* is set to zero.
[g]Present theory. [h]Result from [23]. [i]Result from [28]. [j]E^* is set to zero. [k]Present theory.

Table 5 Dimensions and material properties

	Problem I	Problem II	Problem III
		Elastic layers	
Young's modulus	$E_1 = E_3 = 207 \times 10^9$ N/m^2	$E_1 = E_3 = 207 \times 10^9$ N/m^2	$E_1 = E_3 = 207 \times 10^9$ N/m^2
Density	$\rho_1 = \rho_3 = 7800$ kg/m^3	$\rho_1 = \rho_3 = 7800$ kg/m^3	$\rho_1 = \rho_3 = 7800$ kg/m^3
Thickness	$h_1 = 0.25$ mm	$h_1 = 0.25$ mm	$h_1 = 0.25$ mm
	$h_3 = 2.5$ mm	$h_3 = 2.5$ mm	$h_3 = 2.5$ mm
		Viscoelastic layer	
Shear modulus	$G_2 = 2.615 \times 10^5$ N/m^2	$G_2 = 4.0 \times 10^6$ N/m^2	$G_2 = 20.0 \times 10^6$ N/m^2
Density	$\rho_2 = 2000$ kg/m^3	$\rho_2 = 2000$ kg/m^3	$\rho_2 = 2000$ kg/m^3
Thickness	$h_2 = 1.25$ mm	$h_2 = 1.25$ mm	$h_2 = 1.25$ mm
Core loss factor	$\eta_2 = 0.38$	$\eta_2 = 0.38$	$\eta_2 = 0.38$
	$\nu = 0.3$		
		Whole beam	
Length	$L = 300$ mm	$L = 242.5$ mm	$L = 1084.498$ mm

Table 6 Results for fully covered beams

	Mode 1		Mode 2		Mode 3		Mode 4	
	w_n	η	w_n	η	w_n	η	w_n	η
				Problem I				
Lall et al. [18]	740.56	0.44790×10^{-2}	2948.29	0.11470×10^{-2}	6629.66	0.51209×10^{-3}	11,782.60	0.28850×10^{-3}
Kung and Singh [22]	741	0.45×10^{-2}	2948	0.11×10^{-2}	6630	0.51×10^{-3}	11,783	0.29×10^{-3}
Gao and Liao [32]	740.6	0.45×10^{-2}	2949.0	0.11×10^{-2}	6629.7	0.513×10^{-3}	11,783.0	0.289×10^{-3}
Yang et al. [30]	741	0.45×10^{-2}	2952	0.11×10^{-2}	6647	0.51×10^{-3}	——	——
Mead and Markus [4]	740.564	0.44819×10^{-2}	2949.00	0.11478×10^{-2}	6629.67	0.51243×10^{-3}	11,782.60	0.28870×10^{-3}
Tang and Lumsdaine [25] ($E_2 = 0$)	740.564	0.44819×10^{-2}	2949.00	0.11478×10^{-2}	6629.67	0.51243×10^{-3}	11,782.60	0.28870×10^{-3}
($E_2 \neq 0$)	740.564	0.44825×10^{-2}	2949.00	0.11484×10^{-2}	6629.68	0.51306×10^{-3}	11,782.61	0.28932×10^{-3}
				Problem II				
Lall et al. [18]	1187.93	0.34250×10^{-1}	4573.05	0.10677×10^{-1}	10207.19	0.49577×10^{-2}	18093.87	0.28324×10^{-2}
Mead and Markus [4]	1187.96	0.34261×10^{-1}	4573.08	0.10682×10^{-1}	10207.22	0.49597×10^{-2}	18093.90	0.28336×10^{-2}
Tang and Lumsdaine [25] ($E_2 = 0$)	1187.96	0.34261×10^{-1}	4573.08	0.10682×10^{-1}	10207.22	0.49597×10^{-2}	18093.90	0.28336×10^{-2}
($E2 \neq 0$)	1187.98	0.34271×10^{-1}	4573.14	0.10691×10^{-1}	10207.35	0.49693×10^{-2}	18094.13	0.28431×10^{-2}
				Problem III				
Lall et al. [18]	81.73	0.15839×10^{-1}	309.35	0.45758×10^{-1}	652.85	0.65921×10^{-1}	1097.01	0.76079×10^{-1}
Mead and Markus [4]	81.730	0.15838×10^{-1}	309.35	0.45758×10^{-1}	652.85	0.65921×10^{-1}	1097.01	0.71608×10^{-1}
Tang and Lumsdaine [25] ($E_2 = 0$)	81.730	0.15838×10^{-1}	309.35	0.45758×10^{-1}	652.85	0.65921×10^{-1}	1097.01	0.71608×10^{-1}
($E_2 \neq 0$)	81.742	0.15966×10^{-1}	309.39	0.45877×10^{-1}	652.92	0.66024×10^{-1}	1097.10	0.71694×10^{-1}

Table 7 Results for a simply supported beam

Freq. no.	Present	Howson and Zare [33]	Mead and Markus [4]	Ahmed [34]	Ahmed [35]	Sakiyama et al. [36]	Kameswara Rao et al. [37]	Marur and Kant [38]
1	57.1359	57.1358	57.1359	55.5	57.5	56.159	57.068	57.041
2	219.585	219.585	219.585	——	——	215.82	218.569	218.361
3	465.173	465.172	465.173	451	467	457.22	460.925	460.754
4	768.178	768.177	768.178	——	——	755.05	757.642	758.692
5	1106.69	1106.68	1106.69	1073	1111	1087.9	1086.955	1097.055
6	1465.11	1465.10	1465.11	——	——	1440.3	1433.920	1457.064
7	1833.55	1833.55	1833.55	1779	1842	1802.7	1789.345	1849.380
8	2206.19	2206.19	2206.19	——	——	2169.8	2147.969	2275.916
9	2579.79	2579.79	2579.79	2510	2594	2538.2	——	2562
10	2952.66	2952.65	2952.66	——	——	2906.2	——	——

Table 8 Results for a cantilever beam

Freq. no.	Present	Howson and Zare [33]	Ahmed [34]	Ahmed [35]	Sakiyama et al. [36]	Marur and Kant [38]
1	33.7514	33.7513	32.79	33.97	33.146	33.7
2	198.993	198.992	193.5	200.5	195.96	197.5
3	512.308	512.307	499	517	503.43	505.5
4	907.3	907.299	886	918	893.28	890.5
5	1349.66	1349.65	1320	1368	1328.5	1321
6	1815.82	1815.82	1779	1844	1790.7	1786
7	2292.46	2292.45	2249	2331	2260.2	2271
8	2772.24	2772.23	2723	2824	2738.9	2792

Table 9 Results for a fixed–fixed beam

Freq. no.	Present	Howson and Zare [33]	Sakiyama et al. [36]	Raville et al. [39]
1	34.5966	34.5965	33.563	——
2	93.1000	93.1000	90.364	——
3	177.155	177.155	172.07	185.5
4	282.785	282.784	274.91	280.3
5	406.325	406.325	395.42	399.4
6	544.332	544.331	530.34	535.2
7	693.787	693.787	676.85	680.7
8	852.153	852.153	832.43	867.2
9	1017.35	1017.35	995.36	1020
10	1187.71	1187.70	1163.9	1201

Table 10 Maximum values of η for different values of core loss factor and Y

Core loss factor	Analysis	$Y = 1$		$Y = 13$	
		η	g_{opt}	η	g_{opt}
0.01	Mead and Markus [4]	$168e-3$	——	5.6e-3	——
	Tang and Lumsdaine [25]	$1680e-3$	28.82	5.59e-3	11.22
0.1	Mead and Markus [4]	$1.68e-2$	——	5.6e-2	——
	Tang and Lumsdaine [25]	$1.676e-2$	28.68	5.58e-2	11.16
0.3	Mead and Markus [4]	$4.9e-2$	——	0.165	——
	Tang and Lumsdaine [25]	$4.93e-2$	27.59	0.1652	10.74
1.0	Mead and Markus [4]	0.14	——	0.49	——
	Tang and Lumsdaine [25]	0.140	20.29	0.487	7.888

Table 11 Dimensions and material properties for the validation study

Elastic layers	
Young's modulus	$E_1 = E_3 = 6.89 \times 10^{10}$ N/m^2
Density	$\rho_1 = \rho_3 = 2710$ kg/m^3
Thickness	$h_1 = 0.1$ mm $h_3 = 0.5$ mm
Viscoelastic layer	
Poisson's ratio	$\nu = 0.4$
Density	$\rho_2 = 1000$ kg/m^3
Thickness	$h_2 = 0.054965$ mm
Core loss factor	$\eta_2 = 0.7$
Whole beam	
Length	$L = 150$ mm

$$(B_1B_3 - B_2^2)k^{*6} - B_1Y_T^*g_T^*k^{*4} - \frac{mL^4}{D^*}\Omega^{*2}(B_3k^{*2} - Y_T^*g_T^*) = 0 \tag{39}$$

$$m_3L^4\Omega^{*2} - E_3I_3k^{*4} = 0 \tag{40}$$

where the complex frequency factor Ω^*, frequency Ω, and loss factor η are related by [2]

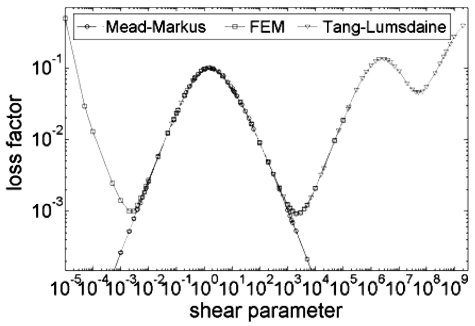

Fig. 4 Comparison of theory with continuum finite elements and Mead–Markus model.

$$\Omega^{*2} = \Omega^2(1 + j\eta) \tag{41}$$

Equation (39) is a cubic equation in k^{*2}, and so the roots can be expressed in the simpler form $\pm k_1^*$, $\pm k_2^*$, and $\pm k_3^*$. Then Eq. (38) can be expressed as

$$w = (A_1e^{k_1^*\bar{x}} + A_2e^{-k_1^*\bar{x}} + A_3e^{k_2^*\bar{x}} + A_4e^{-k_2^*\bar{x}} + A_5e^{k_3^*\bar{x}} + A_6e^{-k_3^*\bar{x}})e^{j\Omega^* t} \tag{42}$$

$$w_u = (B_1e^{k_4\bar{x}} + B_2e^{-k_4\bar{x}} + B_3e^{ik_4\bar{x}} + B_4e^{-ik_4\bar{x}})e^{j\Omega^* t} \tag{43}$$

where $A_1, \ldots, A_6$ and $B_1, \ldots, B_4$ are constants to be determined from boundary equations (21) and (27–29) and Table 1. Then the equations so formed can be expressed in matrix form $[x](A) = (0)$. For a nontrivial solution, the determinant of x should be zero. The real part and imaginary part of the complex frequency factor Ω^* are the variables to be determined for this problem. These must be determined numerically for all boundary conditions (except for the simply supported fully covered case, in which a closed solution is possible).

This problem is solved using two different methods. Typically, a gradient-based optimization program is used. The objective function is the absolute value of the determinant, which is to be minimized. The problem is solved using a commercial optimization subroutine. The subroutine uses a quasi-Newton method from the IMSL commercial software package. A genetic algorithm is occasionally used. The advantage of using this algorithm is that there is no need for a gradient calculation. The disadvantages are a substantially higher computational time to come to a solution and a sensitivity to setting a proper search interval that sometimes prevents convergence. However, it was found that for very low and very high values of g, the gradient-based method was unable to converge, and so the genetic algorithm was used in these cases.

IV. Validation

A. Fully Covered Beam

First, these results are compared with previously published results for a fully covered beam. The material properties and dimensions used for this validation are listed in Table 2. The results are compared

with an exact theory developed by Daya and Potier-Ferry [28], Johnson et al. [29], Macé [27], Fasana and Marchesiello [6], Yang et al. [30], and Shi et al. [31] are shown in Tables 3 and 4, in which the loss parameter can be defined by

$$\bar{\eta} = \frac{\eta}{\eta_2} = \frac{\text{loss factor of sandwich beam}}{\text{core loss factor}}$$

It can be seen that the results are virtually identical for a variety of core loss factors and for higher modes. The difference of loss parameters between the present theory and the Mead–Markus model is small. The normal strain in the length direction in the viscoelastic layer could be neglected for this case because the shear-parameter value is small.

Another validation is performed using the material properties and dimensions listed in Table 5 [18]. The three beams for this validation (problems I, II, and III) come from Lall et al. [18]. The results are compared with Lall et al. [18], Kung and Singh [22], Tang and Lumsdaine [25], and Gao and Liao [32] and are shown in Table 6. The exact formulation for a simply supported beam from Mead and Markus [4] is used.

A simply supported sandwich beam is analyzed. The dimensions and material properties are as follows: $E_1 = E_3 = 68.9$ GPa, $G_2 = 82.68$ MPa, $\rho_1 = \rho_3 = 2680$ kg/m^3, $\rho_2 = 32.8$ kg/m^3, $2h_1 = 2h_3 = 0.4572$ mm, $2h_2 = 12.7$ mm, and $L = 914.4$ mm. The results are compared with numerous sources in the literature and are shown in Table 7. The present analytical formulation compares well with the other sources for multiple modes.

A cantilever sandwich beam is analyzed. The dimensions and material properties are as follows: $E_1 = E_3 = 68.9$ GPa, $G_2 = 82.68$ MPa, $\rho_1 = \rho_3 = 2680$ kg/m^3, $\rho_2 = 32.8$ kg/m^3, $2h_1 = 2h_3 = 0.4572$ mm, $2h_2 = 12.7$ mm, and $L = 711.2$ mm. The results are compared with numerous sources in the literature and are shown in Table 8. The present analytical formulation again compares well with the other sources for multiple modes.

A fixed–fixed sandwich beam is analyzed. The dimensions and material properties are as follows: $E_1 = E_3 = 68.9$ GPa, $G_2 = 68.9$ MPa, $\rho_1 = \rho_3 = 2687.3$ kg/m^3, $\rho_2 = 119.69$ kg/m^3, $2h_1 = 2h_3 = 0.40624$ mm, $2h_2 = 6.3475$ mm, and $L = 1218.72$ mm. The results are compared with numerous sources in the literature and are shown in Table 9. Raville et al.'s [39] results are experimental. The present analytical formulation again compares well with the other sources for multiple modes.

Mead and Markus [4] also published results for a fully covered fixed–fixed beam. The comparison is shown in Table 10. The differences between the Mead–Markus theory and the present theory are less than 1%. The g_{opt} given in the table is the optimal shear parameter for maximal loss factor.

All preceding validations are cases in which the longitudinal normal strains in the damping layer are negligible. To verify the accuracy of the model when these normal strains are significant, these analytic results are compared with finite element results. The commercial software ABAQUS is used for the finite element analysis. Two-dimensional quadratic continuum plane stress elements CPS8 are used (which include all 3 in-plane stress components). The material properties and dimensions are listed in Table 11. The results are shown in Fig. 4. It is shown that the Mead–Markus model matches the finite element results for g values between 10^{-2} and 10^3. The model presented here (labeled "Tang–Lumsdaine" in the figure) matches the finite element results over this same range, but continues to correlate for g values past 10^5 in a range in which the normal strain in the damping layer becomes significant. It is worth noting that neither the Mead–Markus model nor the Tang–Lumsdaine model match the finite element result for g values below

Table 12 Dimensions and material properties for finite element validation study

Elastic layers	
Young's modulus	$E_1 = E_3 = 6.89 \times 10^{10}$ N/m^2
Density	$\rho_1 = \rho_3 = 2710$ kg/m^3
Thickness	$h_1 = 0.1, 0\ldots25, 0.5$ mm
	$h_3 = 0.5$ mm
Viscoelastic layer	
Young's modulus	$E_2 = 2.8 \times 10^6$ N/m^2
Poisson's ratio	$\nu = 0.4$
Density	$\rho_2 = 1000$ kg/m^3
Thickness	$h_2 = 0.0635$ mm
Core loss factor	$\eta_2 = 0.7$
Whole beam	
Length	$L = 150$ mm

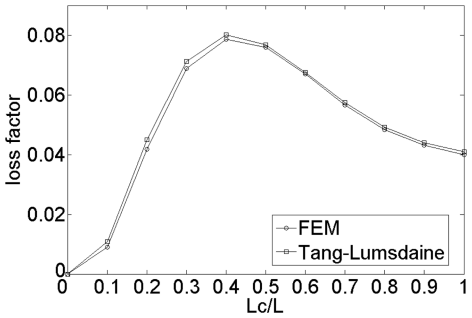

Fig. 5 Comparison of theory with continuum finite elements, $h_1 = 0.1$ mm.

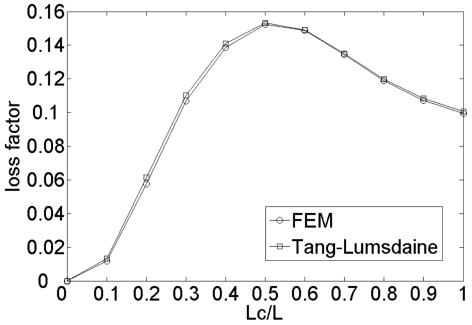

Fig. 6 Comparison of theory with continuum finite elements, $h_1 = 0.25$ mm.

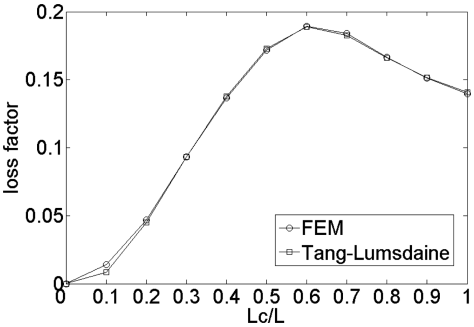

Fig. 7 Comparison of theory with continuum finite elements, $h_1 = 0.5$ mm.

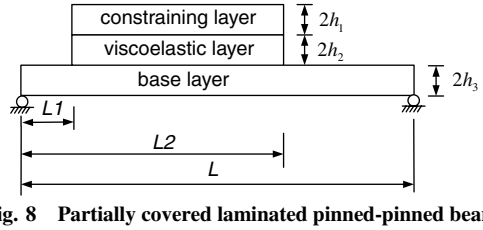

Fig. 8 Partially covered laminated pinned-pinned beam.

Table 13 Results for problem I [15]

	L_1/L	L_2/L	L_1/L	L_2/L	L_1/L	L_2/L
	0	0.2	0	0.4	0	0.6
Position	w_n	η	w_n	η	w_n	η
Lall et al. [18]	811.052	0.61433×10^{-5}	789.194	0.16660×10^{-3}	759.374	0.92948×10^{-3}
Kung and Singh [22]	811.000	0.63000×10^{-5}	788.000	0.17000×10^{-3}	759.000	0.95000×10^{-3}
Gao and Liao [32]	811.000	0.63800×10^{-5}	788.000	0.17400×10^{-3}	759.000	0.95000×10^{-3}
Tang and Lumsdaine [25] ($E_2 = 0$)	810.933	0.63098×10^{-5}	788.449	0.17322×10^{-3}	758.735	0.94653×10^{-3}
($E_2 \neq 0$)	810.933	0.63608×10^{-5}	788.449	0.17354×10^{-3}	758.736	0.94715×10^{-3}

Table 14 Results for problem I [15]

	L_1/L	L_2/L	L_1/L	L_2/L	L_1/L	L_2/L
	w_n	η	w_n	η	w_n	η
Position	0.2	0.4	0.15	0.55	0.1	0.7
Lall et al. [18]	792.963	0.39799×10^{-4}	767.663	0.36266×10^{-3}	748.437	0.12430×10^{-2}
Gao and Liao [32]	792.000	0.41200×10^{-4}	767.000	0.37200×10^{-4}	748.000	0.13000×10^{-4}
Tang and Lumsdaine [25] ($E_2 = 0$)	792.478	0.40879×10^{-4}	766.884	0.36997×10^{-3}	748.108	0.12516×10^{-2}
($E2 \neq 0$)	792.478	0.41150×10^{-4}	766.885	0.37055×10^{-3}	748.109	0.12523×10^{-2}

Table 15 Results for problem I [15]

	L_1/L	L_2/L	L_1/L	L_2/L	L_1/L	L_2/L
	w_n	η	w_n	η	w_n	η
Position	0.4	0.6	0.3	0.7	0.2	0.8
Lall et al. [18]	782.209	0.60001×10^{-4}	767.663	0.36266×10^{-3}	744.300	0.13612×10^{-2}
Gao and Liao [32]	782.000	0.61100×10^{-4}	758.000	0.45600×10^{-4}	744.000	0.14000×10^{-4}
Tang and Lumsdaine [25] ($E_2 = 0$)	781.804	0.60711×10^{-4}	757.660	0.45312×10^{-3}	744.177	0.13644×10^{-2}
($E_2 \neq 0$)	781.805	0.61108×10^{-4}	757.660	0.45380×10^{-3}	744.178	0.13652×10^{-2}

Table 16 Results for problem III [15]

		Lall et al. [18]		Tang and Lumsdaine Tang and Lumsdaine [25] ($E_2 = 0$)		($E_2 \neq 0$)	
L_1/L	L_2/L	w_n	η	w_n	η	w_n	η
0	0.2	62.449	0.21851×10^{-2}	62.348	0.19123×10^{-2}	62.348	0.19154×10^{-2}
0	0.4	64.232	0.11690×10^{-1}	63.960	0.11617×10^{-1}	63.962	0.11638×10^{-1}
0	0.6	69.706	0.23385×10^{-1}	69.583	0.22449×10^{-1}	69.588	0.22510×10^{-1}
0.2	0.4	62.943	0.13827×10^{-1}	62.514	0.12026×10^{-1}	62.515	0.12042×10^{-1}
0.15	0.55	66.864	0.23183×10^{-1}	66.586	0.23932×10^{-1}	66.590	0.23978×10^{-1}
0.1	0.7	73.202	0.29530×10^{-1}	72.966	0.28101×10^{-1}	72.971	0.28231×10^{-1}
0.4	0.6	63.240	0.22363×10^{-1}	62.636	0.18505×10^{-1}	62.638	0.18531×10^{-1}
0.3	0.7	68.580	0.31562×10^{-1}	67.994	0.30834×10^{-1}	68.000	0.30895×10^{-1}
0.2	0.8	74.739	0.33470×10^{-1}	74.468	0.30793×10^{-1}	74.476	0.30890×10^{-1}

10^{-2}, as the damping material becomes so compliant that the transverse normal stresses become significant.

B. Partially Covered Beam

The analytic results are compared with finite element results for a partially covered beam. The configuration is fixed–free, as shown in Fig. 1. The material properties and dimensions are listed in Table 12.

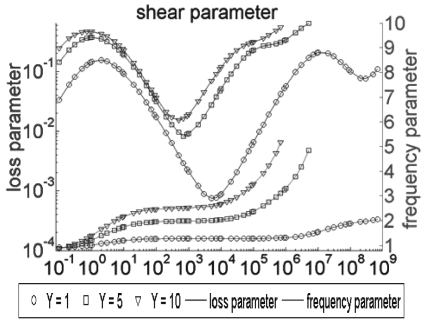

Fig. 9 Loss parameter of fixed–free beam.

The results for different constraining-layer thicknesses are shown in Figs. 5–7. The results are within 2% for L_C/L greater than 0.2. For L_C/L less than 0.2, the error is greater because some of the assumptions of the analysis (such as only shear and longitudinal normal strains existing in the viscoelastic layer) begin to be violated. This confirms the observations of Austin and Inman [23] regarding the limits of the analytic theory for predicting the loss factor in constrained damping layers. In Figs. 5–7, it is seen that the peak damping occurs for a partially covered beam.

A further validation of a partially covered beam is performed for a simply supported beam. The material properties and dimensions used for this validation are listed in Table 5. The configuration is shown in Fig. 8. The two beams (problem I and III) come from Lall et al. [18]. Tables 13–16 show the comparison with the results from Lall et al. [18].

V. Results

A. Fully Covered Beam

Loss parameters and frequency parameters are shown as a function of the shear parameter in Figs. 9–13 for a variety of boundary

conditions (fixed–free, fixed–fixed, fixed–pinned, free–free, and pinned–pinned). The loss parameters and frequency parameters are plotted in these figures for different values of Y. For all cases, the normal strain in the damping layer becomes dominant for higher values of g. It is also notable that as Y increases, the normal strain becomes significant for lower g values. Figure 14 shows the variation of the loss parameter for different core-loss-factor values of the fixed–free beam. It is seen that the core loss factor does not have a significant effect on the loss parameter for low g values, but becomes significant as g increases. This was demonstrated by Rao [40]. However, it is seen that the core loss factor again has no significant effect for the initial region in which normal strain dominates (roughly for g from 10^3 to 10^5), but then becomes significant again for higher g values.

The same problem plotted in Fig. 4 is solved again using the Mead–Markus model (including shear strain only in the viscoelastic), the model developed in this paper (shear and longitudinal normal strain in the viscoelastic layer) and a model for which viscoelastic layer has only longitudinal norm strain. The result is shown in Fig. 15. Comparing with the finite element result, the Mead–Markus model is valid when the shear parameter is small, ($10^{-2} < 10^2$). This means that the viscoelastic layer deforms mostly in shear strain for this range, and normal strains in the length and transverse direction can be neglected. Longitudinal normal strains dominate for large g (greater than 10^4), for which the damping layer becomes stiff. For this range, the shear strain in the viscoelastic layer can be neglected. The present theory is valid for shear parameters from small to large (from $10^{-2}<$ to at least 10^5). This meets the assumption that the beam deflection is the same for three layers; that is, the normal strain in the transverse direction could be neglected. For an extremely small shear parameter, the viscoelastic layer deforms mostly in normal strain in the transverse direction, and so this theory is not applicable.

The effect of beam length is shown in Fig. 16. The three beams (problems I, II, and III) come from Lall et al. [18]. The geometric parameter is the same for the five cases. It is shown that loss parameters are the same using the Mead–Markus model. As the shear parameter increases, the results vary. The ratio of the thickness of the constraining layer to the viscoelastic layer also affects loss parameters. The result is shown in Fig. 17 with the same geometric parameter but different h_1/h_2. When the constraining layer is thicker than the viscoelastic layer, the onset of normal-strain dominance in the damping layer occurs for much higher values of g. The constraining layer prevents normal strain in the viscoelastic layer. So the Mead–Markus model is valid for larger regions for large h_1, as the shearing dominates in the damping layer for a larger range of g values.

When the thickness of the viscoelastic layer is much larger than the constraining layer, normal strain in the transverse direction should be considered. The result is shown in Fig. 18. The difference increases as the loss parameter increases.

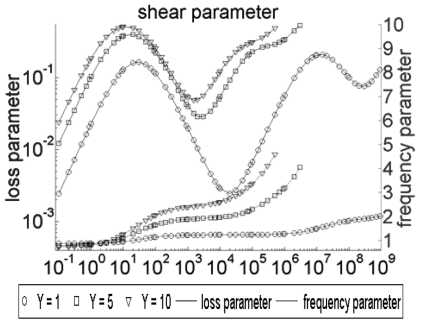

Fig. 10 Loss parameter of fixed–fixed beam.

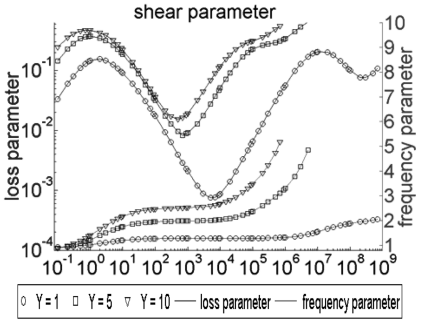

Fig. 11 Loss parameter of fixed–pinned beam.

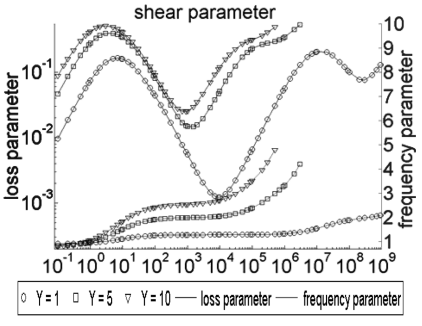

Fig. 12 Loss parameter of free–free beam.

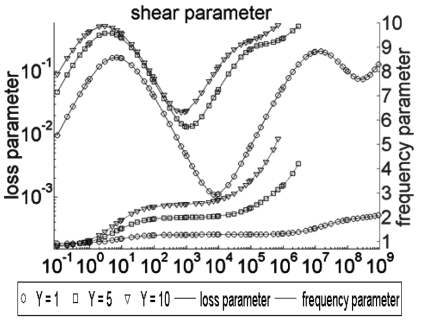

Fig. 13 Loss parameter of pinned–pinned beam.

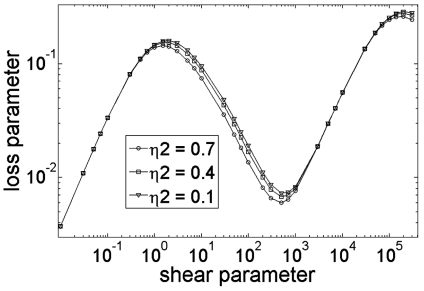

Fig. 14 Loss parameter of fixed–free beam, $Y = 1$.

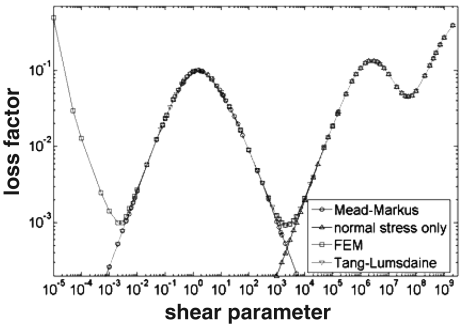

Fig. 15 Loss parameter of fixed–free beam.

B. Partially Covered Beam

A fixed–pinned beam is used to examine a partially covered beam (Fig. 19). The loss parameter vs the shear parameter is shown in Fig. 20 for two different coverage lengths. For certain shear-parameter values, a fully covered beam produces higher damping levels, whereas for other values, a partially covered beam produces higher damping. When the shear parameter is small, a fully covered beam can produce a larger loss parameter than a partially covered beam. As the shear parameter increases, a partially covered beam produces loss parameters greater than a fully covered beam. The loss parameter is plotted versus L_C/L and the shear parameter in Fig. 21. It can be noted that the optimal loss parameter occurs for an L_C/L less than one (that is, maximum damping is always achieved with a partial constraining layer). Figure 22 is the contour plot of Fig. 21. The curve shows the optimal L_C/L with different shear parameters.

Figure 23 shows the surface plot for a cantilever beam. Figure 24 is the contour plot of Fig. 23. It also shows that a partially covered beam can have a loss parameter greater than a fully covered beam.

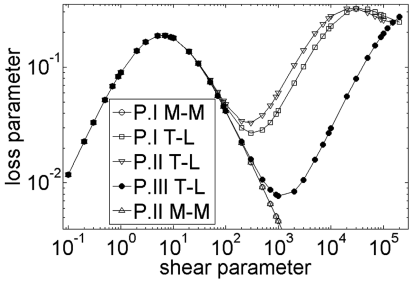

Fig. 16 Loss parameter of pinned–pinned beam.

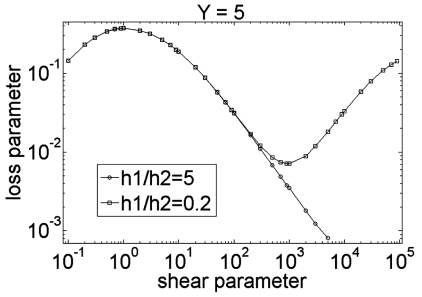

Fig. 17 Loss parameter of a fixed–free beam.

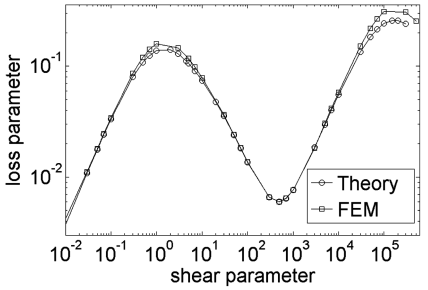

Fig. 18 Loss parameter of a fixed–free beam.

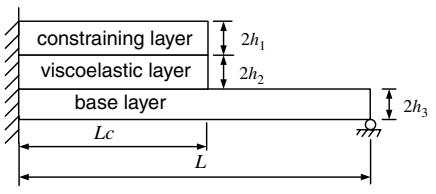

Fig. 19 Partially covered laminated fixed–pinned beam.

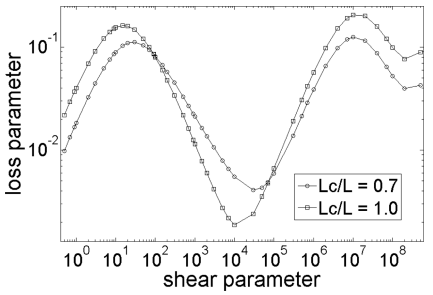

Fig. 20 Loss parameter with different x/L; $x/L = 0.7$ (○) and $x/L = 1.0$ (□).

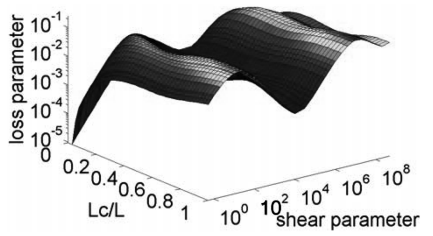

Fig. 21 Loss-parameter surface plot for $Y = 1$.

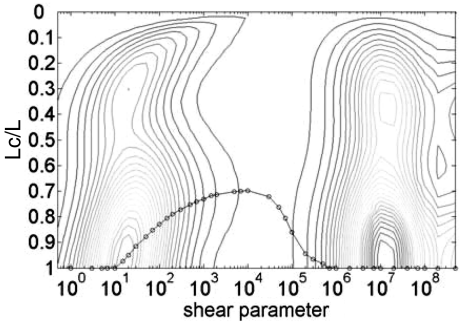

Fig. 22 Loss-parameter contour plot for Fig. 21.

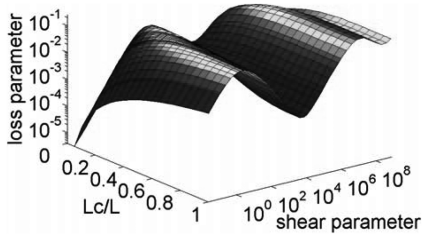

Fig. 23 Loss-parameter surface plot for $Y = 1$.

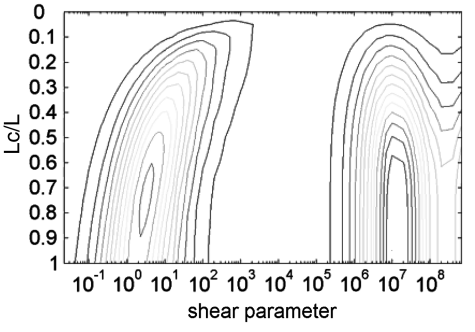

Fig. 24 Loss-parameter contour plot for Fig. 23.

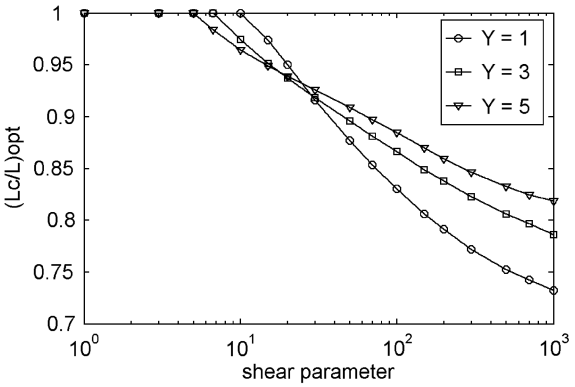

Fig. 25 Optimal L_C/L for fixed–pinned beam.

Figure 25 shows the optimal L_C/L values with different geometric parameter values for a fixed–pinned beam. For a certain range, increasing the shear parameter decreases the optimal covering length. Thus, when the viscoelastic layer is stiffer, the optimal covering length should be shorter. The figure could be used to determine the optimal coverage length for any shear-parameter value for maximum loss factor.

VI. Conclusions

The present work shows a derivation of the equations of motion and boundary conditions for a partial constrained-damping-layer beam for which normal strain in the length direction and shear strain in the viscoelastic layer are considered. This new model can predict loss parameters for larger shear-parameter values. It also can be used to calculate loss parameters for small shear-parameter values as the Mead–Markus model does. The Mead–Markus model is a special case of this model when E_2^* is set to zero. The loss parameter is a function of seven parameters: the shear parameter g_T; the geometric parameter Y_T; the normalized coverage length L_C/L; coefficients B_1, B_2, and B_3; and the core loss factor η_2. Including the normal strain shows another damping peak for cases of high damping-layer stiffness. For most cases, increasing the geometric parameter decreases the optimal covering length. Thus, when the viscoelastic layer is stiffer, the covering length should be shorter to increase damping levels. The plots presented in this paper may be used to design optimal constrained damping layers.

References

[1] Kerwin, E. M., "Damping of Flexural Waves by a Constrained Viscoelastic Layer," *Journal of the Acoustical Society of America*, Vol. 31, No. 7, 1959, pp. 952–962. doi:10.1121/1.1907821

[2] DiTaranto, R. A., "Theory of Vibratory Bending for Elastic and Viscoelastic Layered Finite-Length Beams," *Journal of Applied Mechanics*, Vol. 32, Dec. 1965, pp. 881–886.

[3] Mead, D. J., and Markus, S., "The Forced Vibration of a Three-Layer, Damped Sandwich Beam with Arbitrary Boundary Conditions," *Journal of Sound and Vibration*, Vol. 10, No. 2, 1969, pp. 163–175. doi:10.1016/0022-460X(69)90193-X

[4] Mead, D. J., and Markus, S., "Loss Factors and Resonant Frequencies of Encastre Damped Sandwich," *Journal of Sound and Vibration*, Vol. 12, No. 1, 1970, pp. 99–112. doi:10.1016/0022-460X(70)90050-7

[5] Yan, M. J., and Dowell, E. H., "Governing Equations for Vibrating Constrained Layer Damping of Sandwich Beams and Plates," *Journal of Applied Mechanics*, Vol. 39, No. 4, 1972, pp. 1041–1047.

[6] Fasana, A., and Marchesiello, S., "Rayleigh-Ritz Analysis of Sandwich Beams," *Journal of Sound and Vibration*, Vol. 241, No. 4, 2001, pp. 643–652. doi:10.1006/jsvi.2000.3311

[7] Lee, B. C., and Kim, K. J., "Effects of Normal Strain in Core Material on Modal Property of Sandwich plates," *Journal of Vibration and Acoustics*, Vol. 119, No. 4, Oct. 1997, pp. 493–503. doi:10.1115/1.2889751

[8] Lee, B. C., and Kim, K. J., "Shear and Normal Strain Effects of Core Layers in Vibration of Square Sandwich Plates Under Clamped Boundary Conditions," *Journal of Sound and Vibration*, Vol. 228, No. 4, 1999, pp. 845–856. doi:10.1006/jsvi.1999.2450

[9] Miles, R. N., and Reinhall, P. G., "Effects of Normal Strain in Core Material on Modal Property Of Sandwich Plates," *Journal of Vibration, Acoustics, Stress, and Reliability in Design*, Vol. 108, No. 1, Jan. 1986, pp. 56–64.

[10] Soni, M. L., and Bogner, F. K., "Finite Element Vibration Analysis of Damped Structure," *AIAA Journal*, Vol. 20, No. 5, 1982, pp. 700–707. doi:10.2514/3.51127

[11] Wang, G., and Wereley, N. M., "Spectral Finite Element Analysis of Sandwich Beams with Passive Constraining Layer Damping," *Journal of Vibration and Acoustics*, Vol. 124, July 2002, pp. 376–386. doi:10.1115/1.1469007

[12] Lall, A. K., Asani, N. T., and Nakra, B. C., "Optimum Design of Viscoelastically Damped Sandwich Panels," *Engineering Optimization*, Vol. 6, No. 4, 1983, pp. 197–205. doi:10.1080/03052158308902470

[13] Lifshitz, J. M., and Leibowitz, M., "Optimal Sandwich Beam Design for Maximum Viscoelastic Damping," *International Journal of Solids and Structures*, Vol. 23, No. 7, 1987, pp. 1027–1034. doi:10.1016/0020-7683(87)90094-1

[14] Lumsdaine, A., and Scott, R. A., "Optimal Design Of Constrained Plate Damping Layers Using Continuum Finite Elements," *Proceedings of the 1996 ASME International Mechanical Engineering Congress and Exposition*, American Society of Mechanical Engineers, Noise Control and Acoustics Div., New York, Nov. 1996, pp. 159–168.

[15] Markus, S., "Damping Mechanism of Beams Partially Covered by Constrained Viscoelastic Layer," *Acta Technica CSAV*, Vol. 2, 1974, pp. 197–194.

[16] Nokes, D. S., and Nelson, F. C., "Constrained Layer Damping with Partial Coverage," *Shock and Vibration Bulletin*, Vol. 38, Nov. 1968, pp. 5–10.

[17] Plunkett, R., and Lee, C. T., "Length Optimization for Constrained Viscoelastic Layer Damping," *Journal of the Acoustical Society of America*, Vol. 48, No. 1, 1970, pp. 150–161. doi:10.1121/1.1912112

[18] Lall, A. K., Asnani, N. T., and Nakra, B. C., "Damping Analysis of Partially Covered Sandwich Beams," *Journal of Sound and Vibration*, Vol. 123, No. 2, 1988, pp. 247–259. doi:10.1016/S0022-460X(88)80109-3

[19] Mantena, P. R., Gibson, R. F., and Hwang, S. J., "Optimal Constrained Viscoelastic Tape Lengths for Maximizing Damping in Laminated Composites," *AIAA Journal*, Vol. 29, No. 10, 1991, pp. 1678–1685.

[20] Chen, Q., and Levy, C., "Vibration Analysis of a Partially Covered, Double Sandwich-Type, Cantilever Beam," *Journal of Sound and Vibration*, Vol. 177, No. 1, 1994, pp. 15–29. doi:10.1006/jsvi.1994.1413

[21] Chen, Q., and Levy, C., "Vibration Analysis of a Partially Covered Double Sandwich Cantilever Beam with Concentrated Mass at the Free End," *International Journal of Solids and Structures*, Vol. 31, No. 17, 1994, pp. 2377–2391. doi:10.1016/0020-7683(94)90158-9

[22] Kung, S. W., and Singh, R., "Vibration Analysis of Beams with Multiple Constrained Layer Damping Patches," *Journal of Sound and Vibration*, Vol. 212, No. 5, 1998, pp. 781–805. doi:10.1006/jsvi.1997.1409

[23] Austin, E. M., and Inman, D. J., "Effects of Modeling Assumptions on Loss Factors Predicted for Viscoelastic Sandwich Beams," *Journal of Vibration and Acoustics*, Vol. 122, No. 4, 2000, pp. 434–439. doi:10.1115/1.1287030

[24] Ro, J., and Baz, A., "Optimum Placement and Control of Active Constrained Layer Damping Using Modal Strain Energy Approach," *Journal of Vibration and Control*, Vol. 8, No. 6, 2002, pp. 861–876.

[25] Tang, S.-J., and Lumsdaine, A., "Analysis and Optimization of Partial Constrained Damping Layers," *Adaptive Structures and Material Systems*, Vol. 71, American Society of Mechanical Engineers, New York, Nov. 2006, pp. 213–218.

[26] Crassidis, J. L., Baz, A., and Wereley, N., "H^∞ Control of Active Constraining Layer Damping," *Journal of Vibration and Control*, Vol. 6, No. 1, 2000, pp. 113–136. doi:10.1177/107754630000600106

[27] Macé, M., "Damping of Beam Vibrations by Means of a Thin Constrained Viscoelastic Layer: Evaluation of a New Theory," *Journal of Sound and Vibration*, Vol. 172, No. 5, 1994, pp. 577–591. doi:10.1006/jsvi.1994.1200

[28] Daya, E. M., and Potier-Ferry, M., "A Numerical Method for Nonlinear Eigenvalue Problems Application to Vibrations of Viscoelastic

Structures," *Computers and Structures*, Vol. 79, No. 5, 2001, pp. 533–541.
doi:10.1016/S0045-7949(00)00151-6

[29] Johnson, C. D., Kienholz, D. A., and Rogers, L. C., "Finite Element Prediction of Damping in Structures with Constrained Viscoelastic Layers," *Shock and Vibration Bulletin*, Vol. 51, No. 1, 1981, pp. 71–81.

[30] Yang, W. P., Chen, L. W., and Wang, C. C., "Vibration and Dynamic Stability of a Traveling Sandwich Beam," *Journal of Sound and Vibration*, Vol. 285, No. 3, 2005, pp. 597–614.
doi:10.1016/j.jsv.2004.08.018

[31] Shi, Y., Sol, H., and Hua, H., "Material Parameter Identification of Sandwich Beams by an Inverse Method," *Journal of Sound and Vibration*, Vol. 290, Nos. 3–5, 2006, pp. 1234–1255.
doi:10.1016/j.jsv.2005.05.026

[32] Gao, J. X., and Liao, W. H., "Vibration Analysis of Simply Supported Beams with Enhanced Self-Sensing Active Constrained Layer Damping Treatments," *Journal of Sound and Vibration*, Vol. 280, Nos. 1–2, 2005, pp. 329–357.
doi:10.1016/j.jsv.2003.12.019

[33] Howson, W. P., and Zare, A., "Exact Dynamic Stiffness Matrix for Flexural Vibration of Three-Layered Sandwich Beams," *Journal of Sound and Vibration*, Vol. 282, Nos. 3–5, 2005, pp. 753–767.
doi:10.1016/j.jsv.2004.03.045

[34] Ahmed, K. M., "Dynamic Analysis of Sandwich Beams," *Journal of Sound and Vibration*, Vol. 21, No. 3, 1972, pp. 263–276.
doi:10.1016/0022-460X(72)90811-5

[35] Ahmed, K. M., "Free Vibration of Curved Sandwich Beams by the Method of Finite Elements," *Journal of Sound and Vibration*, Vol. 18, No. 1, 1971, pp. 61–74.
doi:10.1016/0022-460X(71)90631-6

[36] Sakiyama, T., Matsuda, H., and Morita, C., "Free Vibration Analysis of Sandwich Beam with Elastic or Viscoelastic Core by Applying the Discrete Green Function," *Journal of Sound and Vibration*, Vol. 191, No. 2, 1996, pp. 189–206.
doi:10.1006/jsvi.1996.0115

[37] Kameswara Rao, M., Desai, Y. M., and Chitnis, M. R., "Free Vibrations of Laminated Beams Using Mixed Theory," *Composite Structures*, Vol. 52, No. 2, 2001, pp. 149–160.
doi:10.1016/S0263-8223(00)00162-8

[38] Marur, S. R., and Kant, T., "Free Vibration Analysis of Fiber Reinforced Composite Beams Using Higher Order Theories and Finite Element Modeling," *Journal of Sound and Vibration*, Vol. 194, No. 3, 1996, pp. 337–351.
doi:10.1006/jsvi.1996.0362

[39] Raville, M. E., Ueng, E.-S., and Lei, M.-M., "Natural Frequencies of Vibration of Fixed-Fixed Sandwich Beams," *Journal of Applied Mechanics*, Vol. 83, Sept. 1961, pp. 367–371.

[40] Rao, D. K., "Frequency and Loss Factor of Sandwich Beams Under Various Boundary Conditions," *Journal of Mechanical Engineering Science*, Vol. 20, No. 5, 1978, pp. 271–282.
doi:10.1243/JMES_JOUR_1978_020_047_02

E. Livne
Associate Editor